Invited paper

The calculation method of high conversion efficiency THz pulse generation by optical rectification of ultrashort laser pulses with tilted pulse fronts

Lei Yang , Wei Shi * , Lei Hou , Chengang Dong , and Panpan Wang
Applied Physics Department, Xi'an University of Technology, Xi'an, China, 710048
* Email: swshi@mail.xaut.edu.cn

(Received June 1, 2017)

Abstract: The high conversion generation efficiency THz generation through optical rectification using a tilted optical pulse front is described. A calculation method of tilted-pulse-front scheme has detailed descriptions, including the tilt introduced by the grating, increase of the pulse front tilt by demagnification in the imaging of the pulse from the grating onto the generation crystal, and propagation of the tilted intensity front from free-space into the generation crystal. We get an optimal demagnification 3.75 of the imaging system for maximum THz conversion efficiency (□ 0.1519×10^{-3}).

Keywords: Terahertz , Lithium niobate ($LiNbO_3$), Optical rectification, Tilted pulse fronts

doi: 10.11906/TST.054-061.2017.06.03

1. Introduction

The terahertz range (0.1-10*THz*, 30μm-3*mm* in free space, 3cm^{-1} to 330cm^{-1} or 0.4*meV* to 40*meV*) is a unique portion of the electromagnetic spectrum that has so far eluded detailed investigations due to the lack of strong sources [1]. Physical phenomena that can be probed in this spectral range include molecular and material excitations like those in semiconductors, biological molecules and molecular crystals [2-4], charge transfer [5-6] and plasma dynamics [7]. Properties in complex materials, such as the gapped excitations related to superconductivity [8], charge ordering, and hybridization phenomena, phonon and polaron dynamics, and the coherent Drude response related to metal-insulator transitions are processes that terahertz radiation can play a part to help unravel [9]. These remarkable results of THz induced studies clearly show the application potential of intense THz pulses.

The first challenge toward studying the myriad phenomena listed above is a technical one – the development of a reliable source of high-intensity, strong-field terahertz pulses. Optical rectification (OR) of laser pulses has emerged as the most powerful way to generate high- energy THz pulses and resulted in the highest THz pulse energy to date [10-12]. The OR occurs through difference-frequency mixing among the Fourier components that are contained within the spectral bandwidth of the ultrashort optical pulse. Efficient OR requires the group velocity of the ultrashort laser pulse to be equal to the phase velocity of the generated THz radiation. This velocity-matching requirement is conveniently fulfilled in a collinear geometry with ZnTe, and GaP as the nonlinear optical materials for pump wavelengths of around 800*nm* and 1 *μm*, respectively [13]. But the nonlinear coefficients of these materials are far smaller than those of some high dielectric, ferroelectric materials including lithium tantalate ($LiTaO_3$) and lithium niobate ($LiNbO_3$) [14].

In this paper, a velocity matching technique based on tilting the front of the ultrashort excitation pulse has been demonstrated for THz pulse generation by optical rectification. The optimization of tilted-pulse-front scheme was given.

2. Principle of velocity matching by pulse-front tilting

The efficiency of OR depends on matching between the group velocity of the ultrashort light pulse and the phase velocity of the THz radiation. Velocity matching is obtained if the condition

$$v_{THz}^{ph} = v_{opt}^{g} \tag{1}$$

is fulfilled. It was recognized and demonstrated early that the high refractive index values of ferroelectric materials at THz, compared to optical frequencies, results in a THz response that propagates at a very large (Cherenkov) angle $\Theta_C = \cos^{-1}\left(v_{THz}^{ph} / v_{opt}^{gr}\right)$ relative to the optical beam that produces it, where the ratio of phase and group velocities $v_{THz}^{ph} / v_{opt}^{gr}$ is given by that of the group and refractive indexes $n_{opt}^{gr} / n_{THz}^{ph}$ at visible and THz frequencies, respectively.

A tilted pulse front is the key for velocity matching. The THz radiation excited impulsively along this tilted pulse front will propagate according to Huygens' principle perpendicularly to this front with a velocity v_{THz}^{ph}. Although the pump pulse moves with a velocity v_{opt}^{gr}, the projection of this velocity in the propagation direction of the generated THz radiation is only $v_{opt}^{gr} \cdot \cos(\gamma)$. Obviously this projected velocity has to be equal with the velocity of the THz radiation. Therefore instead of Eq. 1, the velocity matching condition reads

$$v_{opt}^{gr} \cdot \cos\gamma = v_{TH}^{p} \tag{2}$$

According to Eq. 2, velocity matching is possible in a material with a significantly larger dielectric constant in the far infrared than in the visible by proper choice of the tilt angle γ [15].

3. Calculation Method of tilted-pulse-front scheme

In a typical experiment, the femtosecond amplified beam is directed onto a grating and the diffracted light is imaged onto the generation crystal. Three main components of the process contribute to the final tilt in the optical beam:

- The tilt of the intensity front imparted by the grating.
- Imaging of the ultrafast pulse incident at the grating onto the generation crystal using a magnification that yields the desired tilt in the pulse front in free-space.
- The change in the tilt of the intensity front upon entering the generation crystal from free-space.

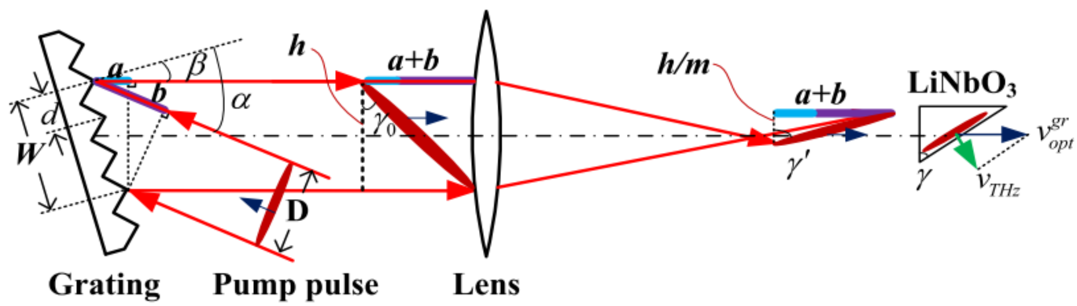

Fig. 1 Experimental setup for THz generation by tilted pulse front excitation. A grating generates a tilted optical pulse front and a lens adjusts the degree of tilt. The LN crystal is cut such that the amplified THz wave reaches the output face at normal incidence and is coupled out.

First let's assume a monochromatic beam of width *h* incident on a grating with groove spacing d of 0.83μm (corresponding to a 1200 *lines/mm* grating typically used for the work done with 800*nm* pump radiation), illuminating a spot of size *W* on the grating. The intensity front of the incident beam is parallel to the phase front of the beam, both of which are along the direction of travel of the beam. The diffraction of the incident beam off the grating follows the grating equation [16]:

$$\sin\alpha + \sin\beta = \frac{\lambda}{d} \tag{3}$$

where λ is the wavelength for a monochromatic beam. The center wavelength of the ultrashort pulses used in the experiments is typically 800*nm*. As illustrated in Figure 1, α is the incident angle of the beam on the grating, and β is the angle at which the beam diffracts off the grating. The + sign in Equation 3 denotes the fact that both the incident and diffracted beams are on the same side of the normal.

Differentiation of Equation 3 with respect to λ yields the angular dispersion:

$$\frac{d\beta}{d\lambda} = \frac{1}{\cos\beta \cdot d} \tag{4}$$

Figure 1 illustrates the pertinent quantities such as *β*, *α*, and *d* which describe the the tilt generated by a diffraction grating. In order to more clearly illustrate how the tilt in the beam is created upon diffraction off the grating, the two sides of the beams are marked with blue and purple hollow circles. Due to the angle at which the grating is oriented, the side of the beam marked with the purple circle travels a distance of *b* (in purple) more than the side marked with the blue circle. Upon diffraction off the grating, the same side travels a distance of *a* (in blue) more than the other. The distances can be written as:

$$a = W\sin\beta$$

$$b = W\sin\alpha$$

Where

$$W = \frac{D}{\cos\alpha}$$

The side of the beam marked with the purple circle thus travels a distance of *a + b* more. This leads to the tilting of the intensity front relative to the phase front which is parallel to the wavevector *k*, determined by the direction of the diffraction beam off the grating. The width of the beam after diffraction is *h*, where:

$$h = W\cos\beta = \frac{D\cos\beta}{\cos\alpha}$$

The resulting tilt of the intensity front can be described by the angle γ_0 where

$$\tan\gamma_0 = \frac{a+b}{h} = \frac{\sin\alpha + \sin\beta}{\cos\beta} = \frac{\lambda}{d\cos\beta}$$

The last equation above relates the angular dispersion to the tilt of the beam in free-space.

Since the angular dispersion $d\beta/d\lambda$ introduced by the grating might not have perfect velocity match for THz generation in LN, the demagnification *M* of the imaging system can be tailored to achieve the desired tilt γ_0 in the image plane on the generation crystal. At the same time, an ultrafast laser pulse that is angularly dispersed upon diffraction off the grating no longer has a short pulse duration since its bandwidth is spatially dispersed. The lens effectively compresses the ultrafast pulse temporally by overlapping the various frequency components spatially at the image plane, which is set to be the surface of the generation crystal.

In the case of a demagnification, *γ* is increased. Figure 1 shows a schematic illustration of the imaging system with a demagnification of *M*. The lens only compresses the dimension parallel to the lens, leaving the dimension along $a+b$ unchanged since this dimension corresponds to the traversal of the tilted pulse in time, and a lens cannot compress along the time dimension. The beam width in the image plane is thus h/M, and the tilt γ_0 is increased to γ':

$$\tan\gamma' = \frac{m(a+b)}{h} = m\tan\gamma_0 = \frac{m\lambda}{d\cos\beta} \tag{5}$$

The tilt also suffers a lateral inversion after passing through a focus in the imaging system.

Finally, the tilt γ in the LN crystal is modified by the group index velocity n_{opt}^{gr} of the material. The effect of n_{opt}^{gr} is a compression along the $a + b$ direction by a factor of n_{opt}^{gr}, since the velocity of light is delayed by n_{opt}^{gr}, in the nonlinear medium [17].

$$\tan\gamma = \frac{m(a+b)}{n_{opt}^{gr} h} = \frac{\tan\gamma'}{n_{opt}^{gr}} \tag{6}$$

4. Experimentation and results

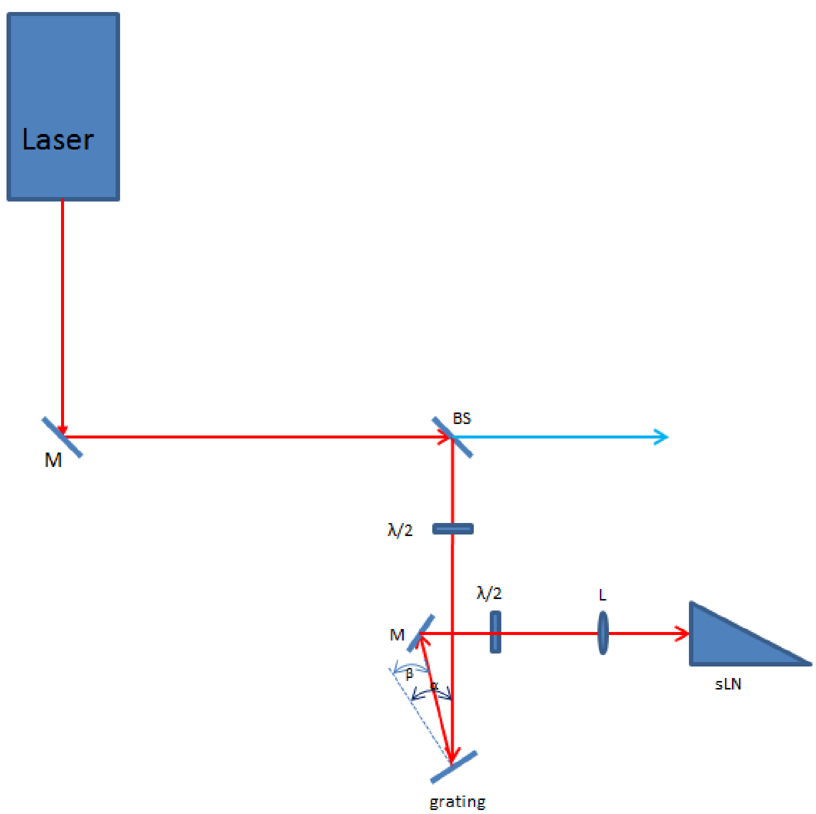

Fig. 2 Experimental setup for THz generation by tilted pulse fronts

Fig. 2 gives the design scheme used in our experiment. The exciting light pulses were obtained from a Ti:sapphire amplifier system laser delivering 100*fs* pulses at 800*nm* with with 0.1*mJ* energy at 1*kHz* repetition rate. A 1200*lines/mm* grating was applied to tilt the intensity front of the pump pulses and a f =100*mm* lens was used to image the spot of the pump beam on the grating into the $LiNbO_3$ crystal. A *λ/2* plate in front of the grating was used to maximize the diffracted efficiency of the grating, while the other *λ/2* plate was used to rotate the polarization of the pump light diffracted from the grating to parallel to the optic axis of LN crystal. A 5.0% MgO-doped congruent LN prism with excitation area of 30×30mm^2 was used for OR. A Golay-cell was used to measure the average power of the THz pulses.

In the case of LN, n_{opt}^{gr}, the optical group index is 2.264 at at 800*nm*, $n_{THz}^{ph} = 5.11$ at 1*THz*, giving $\gamma \approx 63^{\circ}$.

Tab. 1 The corresponding THz generation efficiency as function of the the demagnification M of the imaging system

M (demagnification of the imaging system)	2	2.5	3.	3.5	3.75	3.95	4
α (the incident angle of the beam on the grating)	2.99°	6.22°	10.52°	16.29°	20.00°	23.54°	24.5°
β (the angle at which the beam diffracts off the grating)	65.20°	58.38°	51.02°	42.79°	38.16°	34.08°	33.00°
γ_0 (tilt angle)	66.40°	61.36°	56.76°	52.60°	50.68°	49.21°	48.85°
object distance （*mm*）	300	350	400	450	475	495	500
image distance （*mm*）	150	140	133.33	128.57	126.66	125.31	125
The output voltage of Golay-cell （*V*）	0.5	0.73	0.8	0.9	0.98	0.9	0.8
the average power of the THz pulses （μW）	7.75	11.31	12.4	13.95	15.19	13.95	12.4
THz generation efficiency （10^{-3}）	0.0775	0.1131	0.124	0.1395	0.1519	0.1395	0.124

The corresponding THz generation efficiency as function of the the demagnification M of the imaging system are shown in Table. 1. As can be seen in Table. 1, when the M changes, the incident angle of the beam on the grating α, the angle at which the beam diffracts off the grating β, tilt angle γ_0, object distance, image distance, the output voltage of Golay-cell, the average power of the THz pulses, and THz generation efficiency are changing.

From Table. 1. there is an optimal demagnification M=3.75 of the imaging system for maximum THz conversion efficiency (□ 0.1519×10^{-3}).

5. Conclusions

In conclusion, a calculation method of tilted-pulse-front scheme has detailed descriptions. An optimal demagnification M=3.75 of the imaging system for maximum THz conversion (□ 0.1519×10^{-3}) has also been presented. We will improve the laser power and reduce the temperature of the LN to improve the THz conversion efficiency in the future.

References

[1] Hirori, H., Doi, A., Blanchard, F. & Tanaka, K. “Single-cycle terahertz pulses with amplitudes exceeding 1 MV/cm generated by optical rectification in $LiNbO_3$”. *Appl Phys Lett* 98**,** 2011–2014 (2011).

[2] B. Ferguson and X.-C. Zhang. “Materialsfor terahertz science and technology”. *Nature Mater*. 1 (2002), 26-33 (2002).

[3] B. M. Fischer, M. Walther, and P. U. Jepsen. “Far-infraredvibrationalmodes of DNA components studied by terahertz time-domain spectroscopy”. *Phys. Med. Biol.* 47, 3807-3814 (2002).

[4] M. Walther, B. M. Fischer, and P. U. Jepsen. “Noncovalent intermolecular forces in polycrystalline and amorphous saccharidesin the far infrared”. *Chem. Phys*.288, 261-268 (2003).

[5] M. C. Beard, G. M. Turner, and C. A. Schmuttenmaer. “Terahertz spectroscopy”. *J. Phys. Chem.* B 106, 7146-7159 (2002)

[6] M.-L. Groot, M. H. Vos, I. Schlichting, et al.. “Coherent infrared emission from myoglobin crystals: An electricfield measurement”. *Proc. Natl Acad. Sci*. USA 99, 1323-1328 (2002).

[7] K. Y. Kim, B. Yellampalle, J. H. Glownia, et al.. “Measurements of terahertz electrical conductivity of intense laser-heated dense aluminum plasmas”. *Phy. Rev. Lett*. 100, 135002. (2008).

[8] R. D. Averitt, G. Rodriguez, A. I. Lobad, et al.. “Nonequilibrium superconductivity and quasiparticledynamics in $YBa_2 CU_3 O_{7-\delta}$”. *Phys. Rev. B* 63, 140502 (2001).

[9] D. J. Hilton, R. P. Prasankumar, S. A. Tugman, et al.. “On photo-induced phenomena in complex materials: probing quasiparticledynamics using infrared and far-infraredpulses”. *J. Phys. Soc. Japan* 75, 011006. (2006).

[10] J. Hebling, G. Almasi, I. Kozma, and J. Kuhl. “Velocity matching by pulse front tilting for large area THz-pulse generation”. *Opt. Express* 10(21), 1161–1166 (2002)

[11] J. A. Fülöp, L. Pálfalvi, M. C. Hoffmann, and J. Hebling. “Towards generation of mJ-level ultrashort THz

pulses by optical rectification". *Opt. Express* 19(16), 15090–15097 (2011).

[12] C. Vicario, A. V. Ovchinnikov, S. I. Ashitkov, et al.. "Generation of 0.9- mJ THz pulses in DSTMS pumped by a Cr:Mg_2SiO_4 laser". *Opt. Lett*. 39(23), 6632–6635 (2014).

[13] K.-L. Yeh, M. C. Hoffmann, J. Hebling, and K. A. Nelson. "Generation of 10μJ ultrashort terahertz pulses by optical rectification". *Appl. Phys. Lett*. 90(17), 171121 (2007).

[14] J. A. Fülöp, L. Pálfalvi, G. Almási, and J. Hebling. "High energy THz pulse generation by tilted pulse front excitation and its nonlinear optical applications". *J. Infrared, Millimeter, Terahertz Waves*, 32, 5, 553–561 (2011).

[15] J. A. Fülöp, L. Pálfalvi, G. Almási, and J. Hebling. "Design of high-energy terahertz sources based on optical rectification". *Opt. Express*, 18. 12. 12311–12327 (2010).

[16] J. Hebling. "Derivation of the pulse front tilt caused by angular dispersion". *Opt. Quantum Electron.*, 28, 12, 1759–1763 (1996)

[17] K. L. Yeh. "The generation of high field terahertz radiation and its application in terahertz nonlinear Spectroscopy". *Massachusetts Institute of Technology*, Dept. of Chemistry, 1-80 (2009).